

RESEARCH ARTICLE | OCTOBER 03 2024

## Stretchable, enhancement-mode PEDOT:PSS organic electrochemical transistors

Yan Wang  ; Dingyao Liu; Jing Bai  ; Xinyu Tian  ; P. T. Lai   ; Shiming Zhang  

 Check for updates

*Appl. Phys. Lett.* 125, 141901 (2024)

<https://doi.org/10.1063/5.0230947>



View  
Online



Export  
Citation

# Stretchable, enhancement-mode PEDOT:PSS organic electrochemical transistors

Cite as: Appl. Phys. Lett. **125**, 141901 (2024); doi: [10.1063/5.0230947](https://doi.org/10.1063/5.0230947)

Submitted: 27 July 2024 · Accepted: 20 September 2024 ·

Published Online: 3 October 2024



View Online



Export Citation



CrossMark

Yan Wang, Dingyao Liu, Jing Bai, Xinyu Tian, P. T. Lai, <sup>a)</sup> and Shiming Zhang <sup>a)</sup>

## AFFILIATIONS

Department of Electrical and Electronic Engineering, The University of Hong Kong, Hong Kong SAR, China

<sup>a)</sup>Authors to whom correspondence should be addressed: [laip@eee.hku.hk](mailto:laip@eee.hku.hk) and [szhang@eee.hku.hk](mailto:szhang@eee.hku.hk)

## ABSTRACT

The rise of wearable and implantable bioelectronics necessitates stretchable electronic devices and systems to seamlessly integrate with soft biological environments. Stretchable organic electrochemical transistors (OECTs), based on conducting polymer poly(3,4-ethylenedioxythiophene) doped with polystyrene sulfonate (PEDOT:PSS), have emerged as a promising candidate because of their combined high stability and high transconductance. However, a stretchable, enhancement-mode PEDOT:PSS OECT (SE-OECT) is still missing, limiting the development of complementary and low-power integration systems. In this Letter, we report SE-OECTs. The devices showed typical enhancement-mode transistor behaviors with standby power as low as  $0.1 \mu\text{W}$  while maintaining stable performance after 1000 cyclic tests within 50% strain.

Published under an exclusive license by AIP Publishing. <https://doi.org/10.1063/5.0230947>

The rise of wearable and implantable bioelectronics calls for mechanically soft electronic devices and systems to blur the interface between rigid electronics and soft biological environments.<sup>1–4</sup> In recent years, organic electrochemical transistors (OECTs) have been heavily researched due to their ability to obtain high sensitivity at low power.<sup>5–9</sup> Despite many channel materials that have been proposed, conducting polymer poly(3,4-ethylenedioxythiophene) doped with polystyrene sulfonate (PEDOT:PSS) remains the first choice for OECTs, due to its commercial availability, solution processability, water stability, and wider conductivity range compared to the competing materials.<sup>10–14</sup> Making PEDOT:PSS OECTs mechanically stretchable can facilitate their deployment at soft bioelectronic interfaces and promote the development of emerging soft neuro-electronics.<sup>15–18</sup> However, traditional stretchable PEDOT:PSS OECTs only work in depletion-mode, limiting the development of complementary wearable or integration systems. Stretchable devices capable of working in enhancement-mode can increase energy efficiency by reducing standby power.<sup>19,20</sup> In addition, enhancement-mode devices can significantly decrease the bus current, which is favorable for developing stretchable bio-integrated circuits and systems. Recently, it has been proved that amine-rich polymers can serve as dedopants for PEDOT:PSS by reducing  $\text{PEDOT}^+$  to its neutral state, offering a possible route to develop enhancement-mode OECTs [Fig. 1(a)].<sup>21–24</sup> Nevertheless, stretchable enhancement-mode PEDOT:PSS devices have not been demonstrated so far, necessitating further study on material mechanics after dedoping and exploring more fabrication methods for stretchable devices.<sup>25–28</sup>

In this Letter, we report stretchable, enhancement-mode PEDOT:PSS OECTs (SE-OECTs) [Figs. 1(b) and 1(c)]. The device is assembled by developing (i) a facile solution-processable approach allowing efficient dedoping of stretchable PEDOT:PSS thin films on elastomers and (ii) a two-step annealing process to immobilize the dedopants within the channel without affecting their functionality and stability. The resulting devices could be stretched between 0% and 50% strain and remain functional within 1000 cycles of the stability test.

For the fabrication of SE-OECTs, we started by investigating the efficacy of dedopants for stretchable PEDOT:PSS thin films. To do so, two widely used water-processable dedopants were used: N-(2-aminoethyl)-1,2-ethanediamine (DEMTA) and branched poly(ethyleneimine) (PEI). DEMTA (optimized at 30 v/v. %) was mixed with PEDOT:PSS suspension in an ice bath to avoid gelation. Diluted PEI solution in de-ionized water (optimized at 10 v/v. %) was cast on prepared PEDOT:PSS thin films. Annealing of the films (120 °C, 20 min) was conducted in a nitrogen atmosphere to avoid oxidation of DEMTA and PEI by ambient oxygen.<sup>29</sup>

The dedoping efficiency of DEMTA and PEI for stretchable PEDOT:PSS films prepared on thermoplastic polyurethane (TPU) elastomer is compared in Fig. 2(a). Despite the concentration of PEI being less than that of DEMTA (10 v/v. % vs 30 v/v. %), the conductivity of the resulting film is two orders of magnitude lower, indicating its higher dedoping efficiency. This can be explained because PEI contains a higher density of electron-rich amine/imine sites on each molecule.

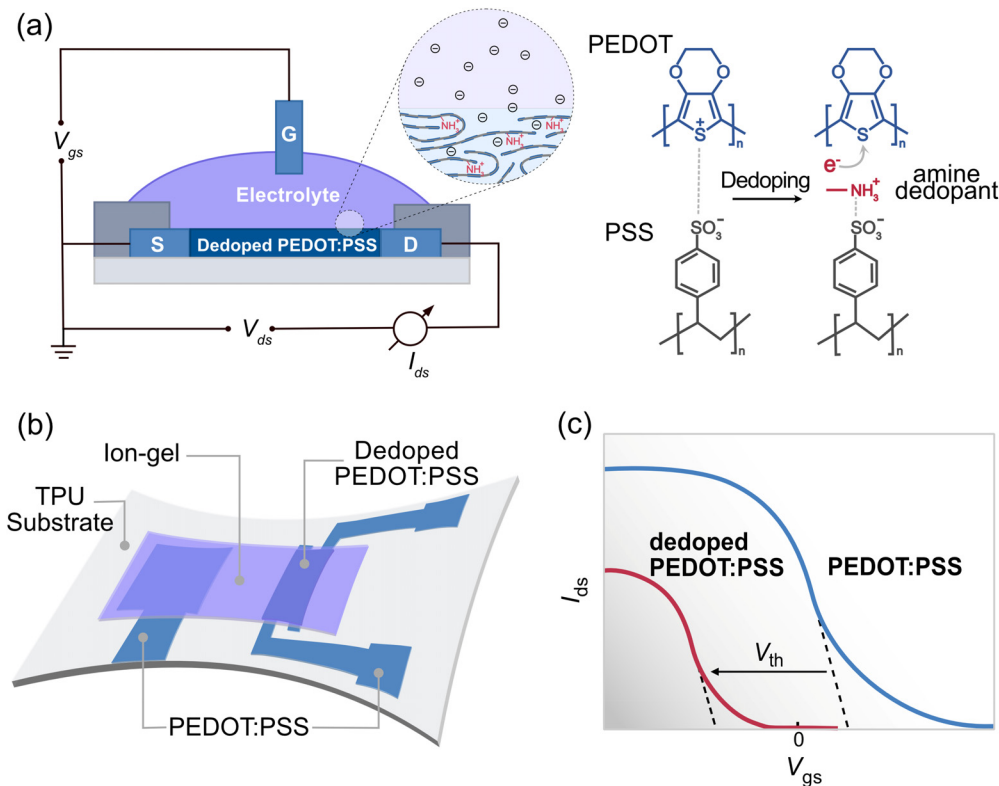


**FIG. 1.** Stretchable, enhancement-mode PEDOT:PSS OECTs (SE-OECTs). (a) Structure of SE-OECTs (left). Dedoping process of PEDOT:PSS (right). (b) Schematic of SE-OECTs. (c) Representative transfer curves of depletion-mode OECTs (pristine PEDOT:PSS) and enhancement-mode OECTs (dedoped PEDOT:PSS).

03 January 2026 11:09:49

Additionally, PEI-doped stretchable PEDOT:PSS thin films also showed better aqueous stability than DEMTA-doped ones [Fig. 2(b)]. We attribute this to the difference in molecular size between DEMTA and PEI. The smaller DEMTA molecules, compared to the long-chain PEI polymers, tend to leak easily from the porous and stretchable PEDOT:PSS channel into water [Fig. 2(c)].

Despite PEI showing superior dedoping efficiency and better aqueous stability, prolonged water immersion (up to 180 h) can still cause a two-order-of-magnitude decrease in resistance ( $10^4$  to  $10^2 \text{ k}\Omega$ ), limiting the practicability to assemble a stretchable device. This issue can be solved by using a crosslinker, such as (3-glycidyloxypropyl) trimethoxysilane (GOPS), to bond PEDOT:PSS and PEI. However, directly mixing PEI and GOPS can result in a loss of functionality for both during annealing process because the amine groups on PEI react with epoxy groups on GOPS.

We solved the above dilemma by developing a two-step annealing method (soft-hard annealing) [Figs. 3(a) and 3(b)]. In the first step, only GOPS (optimized at 2 v/v.%) was mixed with the PEDOT:PSS solution. A soft annealing process ( $80^\circ\text{C}$ , 5 min) was performed to, on the one hand, dry the PEDOT:PSS and partially crosslink it through GOPS and, on the other hand, allow a portion of GOPS to remain reactive. In the second step, PEI (10 v/v.%) was coated on the film, followed by a hard annealing process ( $120^\circ\text{C}$ , 20 min). During the hard annealing process, the remaining reactive GOPS molecules crosslink PEDOT:PSS and PEI, preventing mobilization of the latter, thus

improving aqueous stability. The efficacy of this method is illustrated in Fig. 3(c). The hard-hard annealing process refers to a two-step annealing with both steps performed at high temperatures ( $120^\circ\text{C}$ , 5 min;  $120^\circ\text{C}$ , 20 min). Stretchable films prepared with the soft-hard annealing method remained highly dedoped ( $10^3 \text{ k}\Omega$ ) and showed improved stability after water immersion for 180 h.

Having addressed the stability issues, we then investigated the stretchability of the dedoped film. We found that the dedopant PEI can simultaneously increase the film's stretchability. As shown in Figs. 4(a) and 4(b), PEI-doped films lost only 35% of the initial current under 50% strain, while the reference film lost 70%. The increased stretchability could benefit in the following ways: (i) PEI itself, in addition to being a dopant, can serve as a plasticizer in the PEDOT:PSS film; and (ii) electron-rich PEI could weaken the ionic interaction between  $\text{PEDOT}^+$  and  $\text{PSS}^-$ , promoting the release and elongation of  $\text{PEDOT}^+$  and  $\text{PSS}^-$  chains. Atomic force microscope (AFM) analysis [Fig. 4(c)] confirmed our hypothesis, in which the dedoped PEDOT:PSS film contains more nanofibrous structures (beneficial for stretchability) compared to the pristine PEDOT:PSS film.<sup>30-32</sup>

The SE-OECTs were then fabricated using inkjet printing and soft-hard annealing method. Stretchable, doped PEDOT:PSS thin films (high conductivity) were used as electrodes (source, drain, and gate). Then, PEI was inkjet-printed on the defined channel area (channel width  $W = 2000 \mu\text{m}$ , length  $L = 200 \mu\text{m}$ , thickness  $d = 80 \text{ nm}$ ). An ion-gel was used as the stretchable electrolyte to bridge the channel

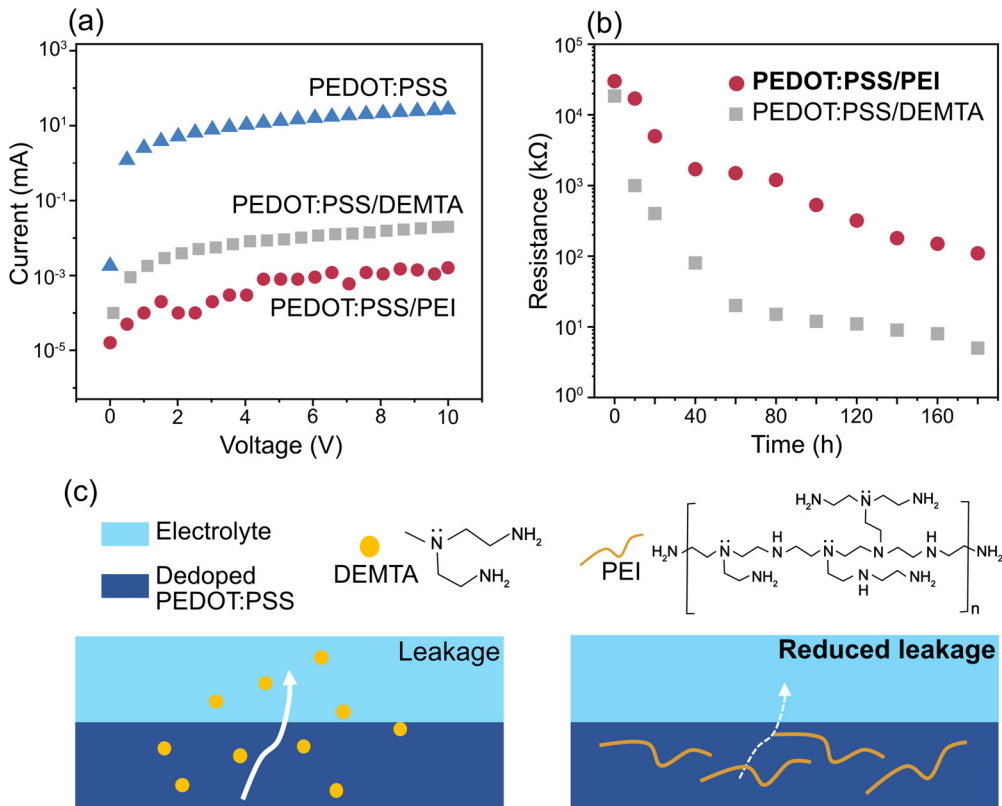


**FIG. 2.** Comparison of aqueous stability of the dedoped PEDOT:PSS films on elastomers. (a) I-V curves of pristine PEDOT:PSS, PEDOT:PSS/DEMTA, and PEDOT:PSS/PEI. (b) Comparison of aqueous stability of PEDOT:PSS/DEMTA and PEDOT:PSS/PEI thin films (1500 rpm  $\times$  60 s). (c) Illustration of leaking tendency of PEDOT:PSS/DEMTA and PEDOT:PSS/PEI channels.

03 January 2024 11:09:49

and the gate [Fig. 1(b)]. The resulting stretchable SE-OECTs showed typical transistor behaviors working in enhancement-mode and remained functional under a strain range of 0%–50% [Figs. 5(a) and 5(b)]. As shown in the transfer curves ( $V_{ds} = -0.6$  V), a low  $I_{ds}$  value of 0.1  $\mu$ A was recorded at  $V_{gs} = 0$  V, which increased to 67  $\mu$ A at  $V_{gs} = -1.5$  V. The transfer curves were reversible and repeatable when  $V_{gs}$  was swept between 0.8 and  $-1.5$  V. In all conditions, the gate current  $I_{gs}$  was below 0.1  $\mu$ A. The maximum transconductance ( $g_{max}$ ) under 0 and 50% strain was 0.15 and 0.12 mS, respectively. Threshold voltages ( $V_{th}$ ) of the devices were calculated to be  $-0.18$  V (0% strain) and  $-0.15$  V (50% strain) [Fig. 5(c)]. Hole mobilities ( $\mu_p$ ) were calculated to be  $0.55 \text{ cm}^2 \text{ V}^{-1} \text{ s}^{-1}$  (0% strain) and  $0.40 \text{ cm}^2 \text{ V}^{-1} \text{ s}^{-1}$  (50% strain) [Fig. 5(c)]. Both values were extracted from the following formula:

$$g_m = \frac{Wd}{L} \mu C^* (V_{th} - V_{gs}), \quad (1)$$

where  $\mu$  is the hole mobility and  $C^*$  is the volumetric capacitance.

To gain insight into the electrochemical and electromechanical stability of the SE-OECTs, we performed transient response [Fig. 5(d)] and cyclic stability tests [Fig. 5(e)]. Stable responses were recorded for 1000 cycles between 0% and 50% strain. Because of the low operation voltage and the relatively small  $I_{ds}$ , the SE-OECTs operated at low power

[Fig. 5(f)]. The on-state power consumptions ( $P$ ) were calculated at a low value of  $39 \mu\text{W}$  (0% strain) and  $36 \mu\text{W}$  (50% strain) ( $V_{gs} = -1.5$  V,  $V_{ds} = -0.6$  V), which were extracted from the following formula:

$$P = V_{ds} \times I_{ds} + V_{gs} \times I_{gs}. \quad (2)$$

Accordingly, the standby power is as low as  $0.06 \mu\text{W}$  (0% strain) and  $0.1 \mu\text{W}$  (50% strain) compared to  $25 \mu\text{W}$  of stretchable depletion-mode PEDOT:PSS OECT (SD-OECT) ( $V_{gs} = 0$  V,  $V_{ds} = -0.6$  V), thanks to the relatively small standby  $I_{ds}$  ( $\sim 0.1 \mu\text{A}$ ) when a  $V_{gs}$  is not applied.

In conclusion, we report stretchable, enhancement-mode PEDOT:PSS OECTs. A specific PEDOT:PSS formulation was identified to simultaneously achieve high dedoping efficiency, long-term aqueous stability, and interface stability. In particular, a soft-hard annealing method was developed to prevent leaking of the dedopant for enhanced device robustness. The SE-OECTs showed typical enhancement-mode transistor behaviors with standby power as low as  $0.1 \mu\text{W}$ . The device showed stable performance after 1000 cyclic tests within 50% strain, thanks to the improved stretchability of the dedoped channel and the robustness of the interfaces. The SE-OECTs enrich the device toolbox for developing low-power and soft organic biosensing and bioelectronic systems.

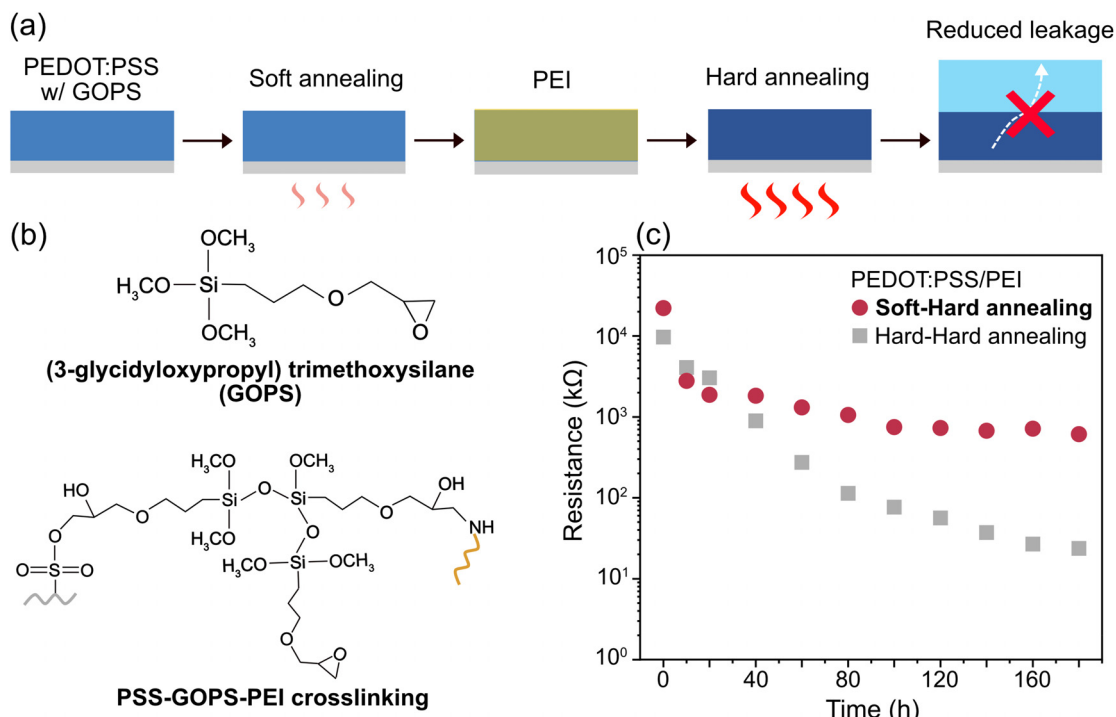


**FIG. 3.** Improving aqueous stability of PEDOT:PSS/PEI thin films by a soft-hard annealing method. (a) Schematics of the soft-hard annealing method. (b) Chemical structures of GOPS and PSS-GOPS-PEI crosslinking after soft-hard annealing. (c) Improved aqueous stability using the soft-hard annealing method.

03 January 2024 11:09:49

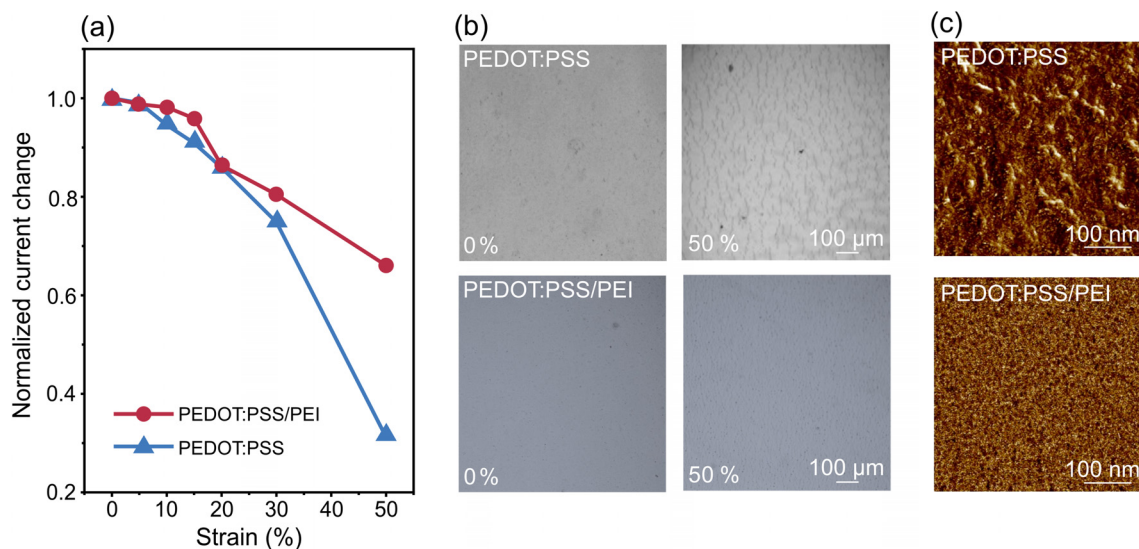


**FIG. 4.** Stretchability enhancement of PEI-dedoped PEDOT:PSS films. (a) Current change of stretchable PEDOT:PSS and PEDOT:PSS/PEI films under different strain values. (b) Microscopic images of stretchable PEDOT:PSS and PEDOT:PSS/PEI films under 0% and 50% strain. (c) AFM phase mapping images of stretchable PEDOT:PSS and PEDOT:PSS/PEI films.

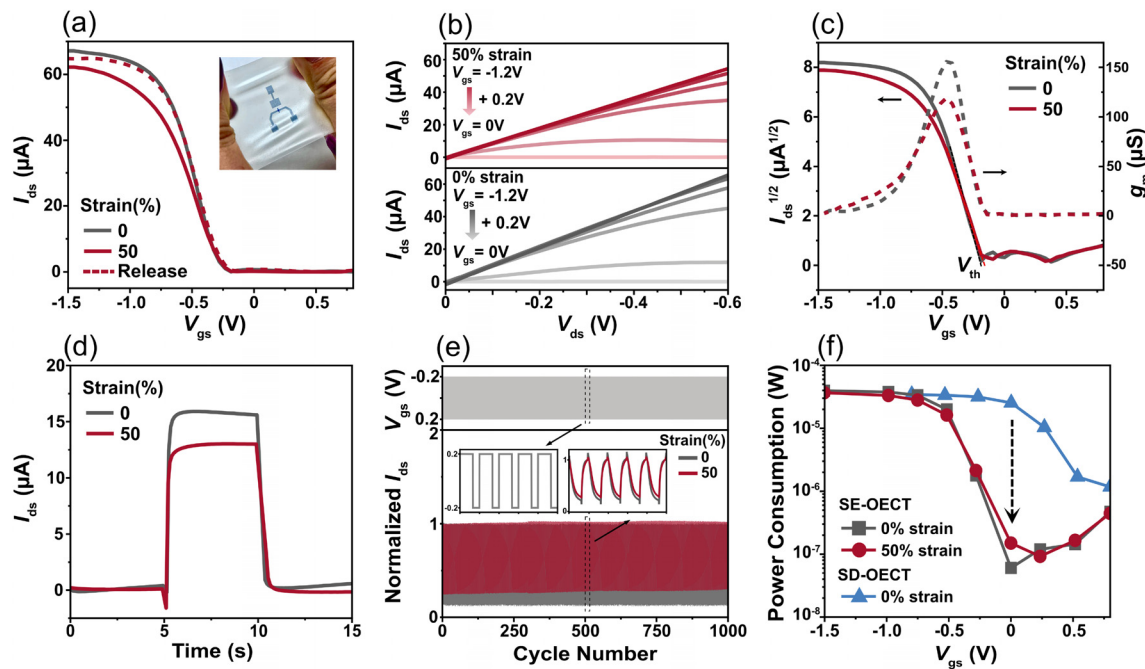


**FIG. 5.** Summary of the electrical performance of SE-OECTs. (a) Transfer curves under 0% (black) and 50% (red) strain.  $V_{ds}$  was fixed at  $-0.6$  V. Inset shows the image of the device under stretching. (b) Output curves at 0% and 50% strain values. (c)  $I_{ds}^{1/2}$ – $V_{gs}$  and  $g_m$ – $V_{gs}$  curves at 0% and 50% strain values. (d) Transient response at 0% and 50% strain values. A pulse of  $V_{gs}$  from 0.2 to  $-0.4$  V was applied. (e) Cyclic stability response (1000 cycles).  $V_{gs}$  was swept between 0.2 and  $-0.2$  V. (f) Comparison of power consumption of SE- and SD-OECTs.

See the [supplementary material](#) for details on the preparation of PEDOT:PSS and PEI inks for inkjet printing.

This work is supported by the Collaborative Research Fund from Research Grants Council of Hong Kong (C7005-23Y), the Innovation and Technology Fund (Mainland-Hong Kong Joint Funding Scheme, MHP/053/21), and Shenzhen-Hong Kong-Macau Technology Research Programme (SGDX20210823103537034).

## AUTHOR DECLARATIONS

### Conflict of Interest

The authors have no conflicts to disclose.

### Author Contributions

Yan Wang and Dingyao Liu contributed equally to this work.

**Yan Wang:** Data curation (lead); Formal analysis (lead); Investigation (lead); Methodology (lead); Validation (lead); Visualization (lead); Writing – original draft (equal); Writing – review & editing (equal).

**Dingyao Liu:** Formal analysis (equal); Investigation (equal); Methodology (equal). **Jing Bai:** Investigation (supporting); Methodology (supporting); Software (supporting). **Xinyu Tian:** Data curation (supporting); Investigation (supporting); Validation (supporting). **P. T. Lai:** Funding acquisition (equal); Supervision (equal); Writing – review & editing (equal). **Shiming Zhang:** Conceptualization (equal); Formal analysis (equal); Funding acquisition (equal); Investigation (equal); Methodology (equal); Project

administration (equal); Resources (equal); Supervision (equal); Writing – original draft (equal); Writing – review & editing (equal).

## DATA AVAILABILITY

The data that support the findings of this study are available from the corresponding authors upon reasonable request.

## REFERENCES

- Rivnay, R. M. Owens, and G. G. Malliaras, *Chem. Mater.* **26**(1), 679 (2014).
- Someya, Z. Bao, and G. G. Malliaras, *Nature* **540**(7633), 379 (2016).
- Gao, S. Emaminejad, H. Y. Y. Nyein, S. Challa, K. Chen, A. Peck, H. M. Fahad, H. Ota, H. Shiraki, and D. Kiriya, *Nature* **529**(7587), 509 (2016).
- Zhang and F. Cicoira, *Nature* **561**(50), 466 (2018).
- Zhang, P. Kumar, A. S. Nouas, L. Fontaine, H. Tang, and F. Cicoira, *APL Mater.* **3**(1), 014911 (2015).
- Friedlein, J. Rivnay, D. H. Dunlap, I. McCulloch, S. E. Shaheen, R. R. McLeod, and G. G. Malliaras, *Appl. Phys. Lett.* **111**(2), 023301 (2017).
- Szymański, D. Tu, and R. Forchheimer, *IEEE Trans. Electron Devices* **64**(12), 5114 (2017).
- Rivnay, S. Inal, A. Salleo, R. M. Owens, M. Berggren, and G. G. Malliaras, *Nat. Rev. Mater.* **3**(2), 17086 (2018).
- Wang, X. Meng, Y. Zhu, H. Ling, Y. Chen, Z. Li, M. C. Hartel, M. R. Dokmei, S. Zhang, and A. Khademhosseini, *IEEE Electron Device Lett.* **42**(1), 46 (2021).
- Groenendaal, F. Jonas, D. Freitag, H. Pielartzik, and J. R. Reynolds, *Adv. Mater.* **12**(7), 481 (2000).
- Zhang, E. Hubis, C. Girard, P. Kumar, J. DeFranco, and F. Cicoira, *J. Mater. Chem. C* **4**(7), 1382 (2016).

<sup>12</sup>S. Zhang, H. Ling, Y. Chen, Q. Cui, J. Ni, X. Wang, M. C. Hartel, X. Meng, K. Lee, and J. Lee, *Adv. Funct. Mater.* **30**(6), 1906016 (2020).

<sup>13</sup>P. Oldroyd, J. Gurke, and G. G. Malliaras, *Adv. Funct. Mater.* **33**(1), 2208881 (2023).

<sup>14</sup>S. Zhang, Y. Chen, H. Liu, Z. Wang, H. Ling, C. Wang, J. Ni, B. Çelebi-Saltik, X. Wang, and X. Meng, *Adv. Mater.* **32**(1), 1904752 (2020).

<sup>15</sup>S. Zhang, E. Hubis, G. Tomasello, G. Soliveri, P. Kumar, and F. Cicoira, *Chem. Mater.* **29**(7), 3126 (2017).

<sup>16</sup>W. Lee, S. Kobayashi, M. Nagase, Y. Jimbo, I. Saito, Y. Inoue, T. Yambe, M. Sekino, G. G. Malliaras, and T. Yokota, *Sci. Adv.* **4**(10), eaau2426 (2018).

<sup>17</sup>D. Liu, X. Tian, J. Bai, Y. Wang, Y. Cheng, W. Ning, P. K. Chan, K. Wu, J. Sun, and S. Zhang, *Adv. Sci.* **9**(29), 2203418 (2022).

<sup>18</sup>J. Chen, W. Huang, D. Zheng, Z. Xie, X. Zhuang, D. Zhao, Y. Chen, N. Su, H. Chen, and R. M. Pankow, *Nat. Mater.* **21**(5), 564 (2022).

<sup>19</sup>W. J. Dally and J. W. Poulton, *Digital Systems Engineering* (Cambridge University Press, 1998).

<sup>20</sup>D. A. Johns and K. Martin, *Analog Integrated Circuit Design* (Wiley, 2008).

<sup>21</sup>T. P. van der Pol, S. T. Keene, B. W. Saes, S. C. Meskers, A. Salleo, Y. van de Burgt, and R. A. Janssen, *J. Phys. Chem. C* **123**(39), 24328 (2019).

<sup>22</sup>S. T. Keene, T. P. van der Pol, D. Zakhidov, C. H. Weijtens, R. A. Janssen, A. Salleo, and Y. van de Burgt, *Adv. Mater.* **32**(19), 2000270 (2020).

<sup>23</sup>Y. Van De Burgt, E. Lubberman, E. J. Fuller, S. T. Keene, G. C. Faria, S. Agarwal, M. J. Marinella, A. Alec Talin, and A. Salleo, *Nat. Mater.* **16**(4), 414 (2017).

<sup>24</sup>C. Cea, G. D. Spyropoulos, P. Jastrzebska-Perfect, J. J. Ferrero, J. N. Gelinas, and D. Khodagholy, *Nat. Mater.* **19**(6), 679 (2020).

<sup>25</sup>M. ElMahmoudy, S. Inal, A. Charrier, I. Uguz, G. G. Malliaras, and S. Sanaur, *Macromol. Mater. Eng.* **302**(5), 1600497 (2017).

<sup>26</sup>A. Häkansson, S. Han, S. Wang, J. Lu, S. Braun, M. Fahlman, M. Berggren, X. Crispin, and S. Fabiano, *J. Polym. Sci., Polym. Phys.* **55**(10), 814 (2017).

<sup>27</sup>T. P. van der Pol, “Controlling the doping level in a conducting polymer for application in enhancement mode organic electrochemical transistors,” Master thesis (Eindhoven University of Technology, 2018).

<sup>28</sup>S. Bontapalle, A. Opitz, R. Schlesinger, S. R. Marder, S. Varughese, and N. Koch, *Adv. Mater. Interfaces* **7**(11), 2000291 (2020).

<sup>29</sup>S. T. Keene, A. Melianas, Y. van de Burgt, and A. Salleo, *Adv. Electron. Mater.* **5**(2), 1800686 (2019).

<sup>30</sup>Y. Wang, C. Zhu, R. Pfattner, H. Yan, L. Jin, S. Chen, F. Molina-Lopez, F. Lissel, J. Liu, and N. I. Rabiah, *Sci. Adv.* **3**(3), e1602076 (2017).

<sup>31</sup>S. Zhang, Y. Li, G. Tomasello, M. Anthonisen, X. Li, M. Mazzeo, A. Genco, P. Grutter, and F. Cicoira, *Adv. Electron. Mater.* **5**(6), 1900191 (2019).

<sup>32</sup>C. Jeong, D. Kim, and F. S. Kim, *Mater. Chem. Phys.* **284**, 126062 (2022).